JACS
JOURNAL OF THE AMERICAN CHEMICAL SOCIETY

ARTICLE

pubs.acs.org/JACS

Synthesis of the Missing Oxide of Xenon, XeO_2, and Its Implications for Earth's Missing Xenon

David S. Brock and Gary J. Schrobilgen*

Department of Chemistry, McMaster University, Hamilton, Ontario L8S 4M1, Canada

Supporting Information

ABSTRACT: The missing Xe(IV) oxide, XeO_2, has been synthesized at 0 °C by hydrolysis of XeF_4 in water and 2.00 M $H_2SO_{4(aq)}$. Raman spectroscopy and $^{16/18}O$ isotopic enrichment studies indicate that XeO_2 possesses an extended structure in which Xe(IV) is oxygen bridged to four neighboring oxygen atoms to give a local square-planar XeO_4 geometry based on an AX_4E_2 valence shell electron pair repulsion (VSEPR) arrangement. The vibrational spectra of $Xe^{16}O_2$ and $Xe^{18}O_2$ amend prior vibrational assignments of xenon doped SiO_2 and are in accordance with prior speculation that xenon depletion from the Earth's atmosphere may occur by xenon insertion at high temperatures and high pressures into SiO_2 in the Earth's crust.

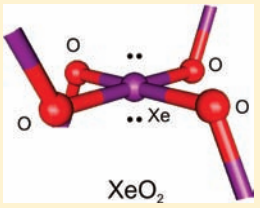

INTRODUCTION

Atmospheric studies of Earth and Mars have shown that xenon is depleted by a factor of approximately 20 relative to the lighter noble gases (Ne, Ar, Kr).[1] More recent studies have found that as much as 90% of the Earth's primordial xenon is absent from its atmosphere,[2] and that more than 99% of xenon has been degassed from the Earth's mantle.[3] It has also been shown that the Earth's core is unlikely to function as a xenon reservoir.[4,5] These findings have aroused the curiosity of researchers from across a broad range of disciplines spanning planetary, mineralogical, geological, nuclear, and other physical sciences as well as theoretical and computational sciences who have attempted to account for atmospheric xenon depletion. Among the explanations that have been advanced to account for xenon depletion are entrapment in ices,[6] water clathrates,[7] sediments,[8] and early escape from the atmosphere;[9] however, all four hypotheses have been shown to be untenable.[6−9] It has also been proposed that xenon displaces silicon from quartz (SiO_2) at the high pressures (0.7−5 GPa) and temperatures (500−1500 K) that are encountered in the continental crust, with the implication that xenon may be retained within silicate minerals and SiO_2 as XeO_2.[10] The high abundance of SiO_2 would make it a significant and readily available reservoir for xenon.

In addition to offering a potential explanation for the Earth's missing xenon, the possible formation of XeO_2 in the Earth's crust is of fundamental chemical interest because XeO_2 represents the missing oxide of xenon. Shortly after the discovery of noble-gas reactivity,[11] solid, colorless XeO_3 was synthesized by hydrolysis of XeF_6 (eq 1)[12,13] and was followed shortly thereafter by the discovery of XeO_4, a pale yellow, volatile solid (eq 2 and 3).[14,15] Both oxides are highly endothermic and shock sensitive (ΔH_f XeO_3, 402 kJ mol^{-1}; ΔH_f XeO_4, 643 kJ mol^{-1}).[16]

$$XeF_6 + 3H_2O \rightarrow XeO_3 + 6HF \quad (1)$$

$$2XeF_6 + 10NaOH \xrightarrow{NaOH_{(aq)}} [Na]_4[XeO_6] + Xe + O_2 + 2H_2O + 6[Na][HF_2] \quad (2)$$

$$[Na]_4[XeO_6] + 2H_2SO_4 \xrightarrow{H_2SO_{4(conc)}} XeO_4 + 2[Na]_2[SO_4] + 2H_2O \quad (3)$$

In contrast, xenon monoxide, XeO, has not been synthesized and has been shown by gas-phase quantum-chemical calculations to have an unstable $^3\Pi$ ground state and, therefore, is unlikely to exist as a monomer.[17] It was initially postulated that the hydrolysis product of XeF_4 was either $Xe(OH)_4$ or $XeO_2 \cdot 2H_2O$,[18] but subsequent studies showed the final product to be XeO_3, which arose from the redox disproportionation given in eq 4.[19,20]

$$4XeF_4 + 8H_2O \xrightarrow{H_2O} 2XeO_3 + 2Xe + O_2 + 16HF \quad (4)$$

Another early study reported the hydrolysis of XeF_4 and the formation of a transient yellow solid at 0 °C. The reaction conditions, which influenced the stability of this species, were optimized by adjusting the acidity of the aqueous medium, but the yellow product was never isolated or characterized.[21] A subsequent study in which XeF_4 and H_2O were co-condensed at −80 °C yielded a pale-yellow product that was incorrectly equated with the aforementioned transient yellow species, and purported to be $XeOF_2$.[22] This proposal was subsequently refuted when $XeOF_2$ was synthesized and definitively characterized, showing the pale-yellow co-condensed product to be a mixture of $XeOF_2$ and $XeOF_2 \cdot n$HF,[23] and by the current study

Received: November 25, 2010
Published: February 22, 2011

dx.doi.org/10.1021/ja110618g | J. Am. Chem. Soc. 2011, 133, 6265–6269

which shows the transient yellow species possesses a Raman spectrum that does not correspond to that of either $XeOF_2$ or $XeOF_2 \cdot nHF$.

RESULTS AND DISCUSSION

In the present study, the aforementioned transient yellow solid was synthesized at 0 °C by the addition of crystalline XeF_4 to either water or 2.00 M $H_2SO_{4(aq)}$. In both cases, intense, yellow-orange suspensions initially formed which, upon mixing for ca. 20 s at 0 °C, produced bright yellow suspensions. The "aged" bright yellow solids are consistent with macromolecular XeO_2 (vide infra) while the initial yellow-orange products are possibly a mixture of molecular XeO_2 and/or lower molecular weight polymorphs resulting from incomplete polymerization (eq 5).

$$nXeF_4 + 2nH_2O \rightarrow \left[nXeO_2 \text{ and/or } \frac{n}{m}(XeO_2)_m \right] + 4nHF \rightarrow (XeO_2)_n + 4nHF \quad (n > m) \qquad (5)$$

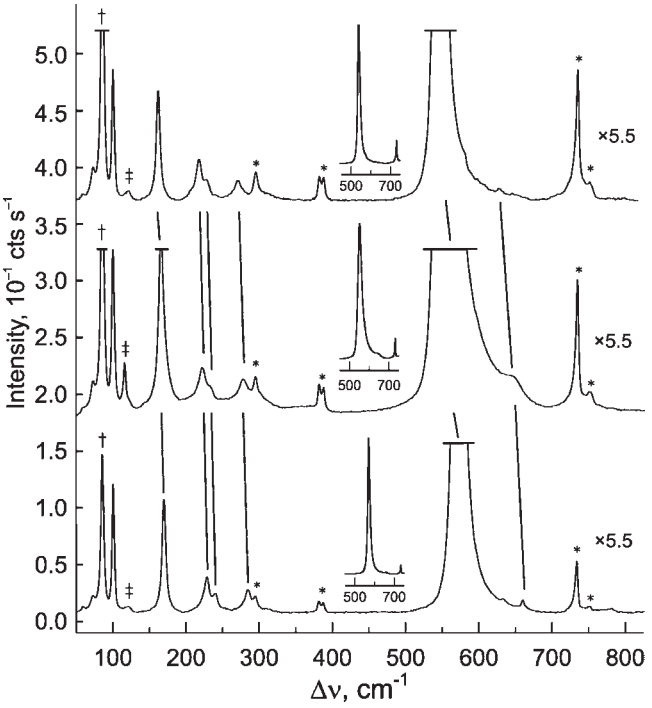

Figure 1. Raman spectra of natural abundance (lower trace), 50% (middle trace), and 97.8% ^{18}O-enriched (upper trace) XeO_2 recorded under frozen water at −150 °C using 1064 nm excitation. Symbols denote FEP sample tube lines (∗), instrumental artifact (†), and minor, incompletely polymerized (yellow-orange) product(s) (‡).

The products were precipitated by briefly centrifuging the reaction mixture at 0 °C followed by immediate quenching at −78 °C and recording the Raman spectrum in situ at −150 °C. At no time were the supernatants discolored, indicating that the yellow products are insoluble in acidified aqueous media. The Raman spectra of the products formed in water and 2.00 M $H_2SO_{4(aq)}$ were identical, indicating that HSO_4^- is not involved in the product.

The yellow product is kinetically stabilized at low temperatures but decomposes rapidly near ambient temperature. At the reaction temperature, 0 °C, the yellow color persisted for ca. 2 min, whereas samples that had been quenched and stored at −78 °C were stable for considerably longer periods with most decomposition occurring over the first 72 h as evidenced by fading of the original color to pale yellow, with a very faint yellow color persisting after 1 week. In each case, Raman spectra of partially decomposed samples revealed only mixtures of the yellow product and small amounts of XeO_3[24] (i.e., the totally symmetric XeO_3 stretch, A_1, was observed as a weak, broad band at 780 cm^{-1}).

Hydrolysis of either $[Cs][XeOF_3]$ or $XeOF_2$ in CH_3CN solvent led to mixtures that also contained the aforementioned yellow product, albeit in smaller amounts (see Hydrolyses of $[Cs][XeOF_3]$ and $XeOF_2$ in the Supporting Information), as evidenced by its characteristic Raman band at 570 cm^{-1} (vide infra).

The yellow species was identified and structurally characterized by Raman spectroscopy using ^{18}O and D isotopic enrichment. Reaction of XeF_4 with $H_2{}^{18}O$ resulted in a Raman spectrum that was similar to that obtained from the reaction of XeF_4 with $H_2{}^{16}O$ (Figure 1); however, all vibrational bands were shifted to lower frequencies (Table 1). The presence of a single, intense band in the Xe−O/Xe−F stretching region and the absence of unshifted modes indicate there are no Xe−F bonds in the compound and that the compound is an oxide and/or hydroxy derivative of Xe(IV).[26] When XeF_4 was allowed to react with $D_2{}^{16}O$, the Raman spectrum of the product was identical to that of $H_2{}^{16}O$ reaction product and devoid of any bands that displayed H/D isotopic dependencies, ruling out a hydroxy compound. The most intense band in the spectrum (570.3 cm^{-1}) is assigned to a symmetric stretching mode that is too low to be associated with the symmetric stretch of XeO_3 (780 cm^{-1})[24] but too high for a Xe(II) oxide fluoride or oxide.[27] The spectrum is therefore

Table 1. Vibrational Frequencies for XeF_4, $Xe^{16}O_2$, $Xe^{16/18}O_2$, and $Xe^{18}O_2$[a]

XeF_4[b]	$Xe^{16}O_2$[c]	$Xe^{16/18}O_2$[c,d]	$Xe^{18}O_2$[c]	D_{2d}[e]	assgnts (L = F, O)[f]
586 ν_6, $\nu(E_u)$	632.3(1)	626.5sh	625.8(1)	ν(E)	$\nu_{as}(XeL_t - XeL_t)$
554 ν_1, $\nu(A_{1g})$	570.3(100)	550.9(100)	542.6(100)	$\nu(A_1)$	$\nu_s(XeL_4)$
524 ν_4, $\nu(B_{2g})$				$\nu(B_2)$	$\nu_{as}(XeL_{2t} - XeL_{2t})$
291 ν_3, $\nu(A_{2u})$	283.9(3)	276.9(2)	270.0(3)	$\nu(B_2)$	$\delta(XeL_4)$ o.o.p., umbrella mode
218 ν_2, $\nu(B_{1g})$	239.1(2)	231sh	226.6(2)	$\nu(B_1)$	$\delta(XeL_{2c} + XeL_{2c})$
	227.9(4)	221.3(4)	216.9(6)		
n.o. ν_5, $\nu(B_{2u})$	n.o.	n.o.	n.o.	$\nu(A_2)$	$\delta(XeL_{2t})$ o.o.p. – $\delta(XeL_{2t})$ o.o.p.
161 ν_7, $\nu(E_u)$[g]	168.9(13)	165.0(19)	161.1(13)	ν(E)	$\delta(XeL_{2t})$ i.p.
	99.5(14)	99.3(17)	99.5(15)		lattice mode

[a] Frequencies are given in cm^{-1}. [b] From ref 25. The symmetries refer to the D_{4h} point symmetry of XeF_4. [c] Values in parentheses denote Raman intensities. [d] The sample was prepared by hydrolysis of XeF_4 in an equimolar mixture of $H_2{}^{16}O$ and $H_2{}^{18}O$. [e] The symmetries refer to the local D_{2d} point symmetry of the XeO_4 units in the extended structure of XeO_2. [f] The abbreviations denote trans (t), cis (c), symmetric (s), asymmetric (as), stretch (ν), bend (δ), in-plane bend (i.p.), and out-of-plane bend (o.o.p.). The in-plane and out-of-plane mode descriptions are relative to the molecular planes of XeF_4 and the XeO_4-unit. [g] This mode was not directly observed. The frequency was obtained from the $2\nu_7$ overtone at 322 cm^{-1}.

dx.doi.org/10.1021/ja110618g | J. Am. Chem. Soc. 2011, 133, 6265–6269

most consistent with the formation of the Xe(IV) oxide, XeO_2. Moreover, monomeric XeO_2 is predicted to have a bent geometry based on an AX_2E_2 (X = bond pair, E = valence electron lone pair) VSEPR[28] arrangement of bond pairs and lone pairs (structure I) and would consequently be a polar molecule. This expectation contrasts with the insolubility of this material in aqueous media, suggesting that XeO_2 likely has an extended (chain or network) structure.

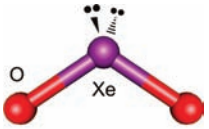

I

The Raman spectra of $Xe^{16}O_2$ and $Xe^{18}O_2$ (Figure 1) also support extended structures. The vibrational frequencies of gas-phase monomeric XeO_2 have been calculated at the CCSD(T) level of theory using the 6-311 g* and aug-cc-PVTZ basis set for oxygen, giving three Raman-active modes at 647 (668), 205 (206), and 703 (716) cm^{-1}, where the aug-cc-PVTZ values are given in parentheses.[29] The bands in the experimental Raman spectra of XeO_2 number six and are broad ($\Delta\nu_{1/2} \approx 20$ cm^{-1}), which is consistent with vibrational coupling and bridge-bonding in an extended structure. A 1:1 molar mixture of $H_2{}^{16}O$ and $H_2{}^{18}O$ was also used to synthesize XeO_2, as described above, in an attempt to resolve the independent spectra corresponding to the $^{16/18}O$ isotopomers of monomeric XeO_2, namely, $Xe^{16}O_2$, $Xe^{16/18}O_2$, and $Xe^{18}O_2$. Instead of three discrete overlapping isotopomeric spectra, the Raman spectrum was comprised of broadened bands that occurred at frequencies that were intermediate with respect to the spectra of $Xe^{16}O_2$ and $Xe^{18}O_2$ (Figure 1 and Table 1). This result is also in accordance with an extended XeO_2 structure in which vibrational coupling extends beyond the primary coordination sphere of xenon. The aforementioned behavior of XeO_2 is not unlike that of SiO_2, which forms discrete monomeric units with double bonds to oxygen in the gas phase, and extended networks in the solid state which display extensive vibrational coupling.[30]

There is a notable similarity between the Raman frequencies of XeO_2 and those of XeF_4 (Table 1), which are in closest agreement for $Xe^{18}O_2$, where the atomic mass of ^{18}O is closest to that of ^{19}F. This leads to the conclusion that the extended XeO_2 structure has a local square-planar geometry for the XeO_4 unit (structure II). The square-planar structural unit is consistent with the VSEPR model of molecular geometry,[28] which is an AX_4E_2 arrangement of four bond pairs and two valence electron lone pairs. This is in accordance with other Xe(IV) compounds which have square-planar (XeF_4,[31] $F_2OXeNCCH_3$,[23] $XeOF_2$,[23] $XeOF_3^-$,[32] $Xe(OTeF_5)_4$[33]) or pentagonal-planar (XeF_5^-,[34] $[XeF_3][SbF_6]$,[35] $[XeF_3][Sb_2F_{11}]$[36]) xenon coordination spheres in the solid state when short secondary contacts are taken into account. However, the bent angles at the oxygen atoms in the extended structure of XeO_2 result in reduction of the local D_{4h} symmetry at xenon and three additional vibrations that are otherwise associated with rotation of the free molecule[37] (see Table S1 in the Supporting Information). The observed bands in the Raman spectrum are most consistent with symmetry lowering to D_{2d} symmetry where the planar XeO_4 moiety is predicted to give rise to nine vibrational bands belonging to the irreducible representations $A_1 + 2A_2 + B_1 + 2B_2 + 3E$, where modes of A_1, B_1, B_2, and E symmetry are Raman active (seven bands); those of B_1, B_2, and E symmetry are infrared active (six bands); and those of A_2 symmetry are Raman and infrared inactive. The vibrational assignments for XeO_2 are therefore made by analogy with the square-planar D_{4h} symmetry of XeF_4 with the understanding that the vibrational mode descriptions under local D_{2d} symmetry will be very similar.

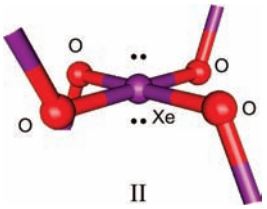

II

The most intense Raman band of XeO_2 occurs at 570.3 cm^{-1} and displays an ^{18}O-isotopic shift of −27.7 cm^{-1}. The band occurs at a frequency that is much lower than the symmetric and asymmetric Xe−O stretches predicted for the gas-phase molecule.[29] This is consistent with coordination of the oxygen atoms to neighboring xenon atoms, which imparts single bond character to the Xe−O bonds and lowers the frequencies of the Xe−O stretching modes. A similar trend has been observed for $XeOF_2$.[23] The 570.3 cm^{-1} band is assigned to the combined $\nu_s(XeO_4)$ and $\nu_{as}(XeO_{2t}{-}XeO_{2t})$ modes, where t denotes oxygen atoms trans to one another. These modes are normally associated with $\nu_1(A_{1g})$ and $\nu_4(B_{2g})$ in an isolated square-planar molecule but are rendered degenerate in an extended lattice (structure II) because the elongation of four Xe−O bonds results in the compression of four Xe−O bonds of the four next nearest neighbor XeO_4 groups. The $\nu_2(B_{1g})$ mode of a square-planar molecule appears as two bands at 227.9 and 239.1 cm^{-1}. These bands exhibit ^{18}O isotopic shifts of −11.0 and −12.5 cm^{-1}, respectively, which are assigned to $\delta(XeO_{2c} + XeO_{2c})$.[38] The extended lattice of XeO_2 also renders modes Raman-active that would otherwise be exclusively infrared active in an isolated centrosymmetric square-planar molecule. A case in point is the weak band at 283.9 cm^{-1}, which is assigned to the out-of-plane XeO_4 bend, $\nu_3(A_{2u})$, and displays a low-frequency shift (−13.9 cm^{-1}) upon ^{18}O-enrichment. Similarly, the otherwise Raman-inactive modes, $XeO_t{-}XeO_t$ and the in-plane bend, XeO_{2t} corresponding to $\nu_6(E_u)$ and $\nu_7(E_u)$, respectively, are observed at 632.3 and 168.9 cm^{-1} with ^{18}O isotopic shifts of −6.5 and −7.8 cm^{-1}, respectively. The out-of-plane coupled bending mode, $\delta(XeO_{2t})$o.o.p.$-\delta(XeO_{2t})$, corresponding to $\nu_5(B_{2u})$, which is formally both Raman and infrared inactive in isolated square-planar centrosymmetric molecules, is also not observed for XeO_2.

The Raman spectrum of the yellow-orange, incompletely polymerized product (Figure S1 in the Supporting Information) is very similar to that of the fully polymerized yellow solid with the exception of a broadened 570 cm^{-1} band, which tails off to higher frequency (~680 cm^{-1}), and a weak band at 310 cm^{-1}. These features may be attributed to shorter oligomers or smaller network structures that have not fully condensed.

Prior work[10] reporting xenon doped SiO_2 has been re-examined in light of the present findings. The study assumed that xenon substitution for silicon in a SiO_2 lattice resulted in xenon occupancy at a tetrahedral site. For this reason, the local xenon geometry was compared with that of XeO_4,[39] assuming that the Xe−O bond lengths and vibrational frequencies of the gas-phase XeO_4 molecule are transferable.[10]

dx.doi.org/10.1021/ja110618g |J. Am. Chem. Soc. 2011, 133, 6265–6269

Consequently, the latter assumption and ensuing comparisons are flawed. The valence shell of Xe(IV) in XeO_2 possesses two valence electron lone pairs. If Xe(IV) were to form bonds to four oxygen atoms in a silicate environment, they would be single bond domains and would adopt a local square-planar AX_4E_2 VSEPR[28] arrangement around Xe(IV) as in structure II. Xenon in tetrahedral XeO_4 is in the +8 oxidation state, forming four double bonds to the oxygen atoms.[39] The prior argument[10] ignores the formal oxidation state of xenon, formal Xe−O single bond orders, and stereochemical activities of the two valence electron lone pairs on Xe(IV). Therefore, the bond lengths and Raman frequencies observed for gas-phase XeO_4 are invalid comparisons. The present arguments are supported by a recent report that provides several calculated models for xenon insertion into SiO_2 networks.[40] One such model positioned xenon at a tetrahedral site which, when energy optimized, gave a local square-planar geometry at xenon. Unfortunately, the steric effects of the free valence electron lone pairs on Xe(IV) and relevant VSEPR arguments were not considered and the optimized square-planar geometry was attributed to packing constraints and stabilization by the surrounding environment.[40]

Thermodynamic considerations in the prior reports of xenon-doped SiO_2[10] attribute the formation of XeO_2 to *PV* work that resulted from an increase in unit cell size and to the high pressures attained in the experiment.[10] The *PV* work was estimated to be −700 kJ mol^{-1}, noting that it "favors the reaction that is otherwise inhibited at ambient conditions because of the high formation enthalpy predicted for XeO_2[29] compared with that of SiO_2." Although −700 kJ mol^{-1} is sufficient to overcome ΔH_f° $XeO_{2(g)}$ (487 kJ mol^{-1}),[29] an ambiguity arises when ΔH_f° $SiO_{2(quartz)}$ (−910.94 kJ mol^{-1})[41] and ΔH_{sub}° $Xe_{(s)}$ (−15.0(2) kJ mol^{-1})[42] are also considered in eq 6, resulting in a highly endothermic (713 kJ mol^{-1}) process when the volume reduction work is included. Equation 6 neglects the lattice enthalpy of XeO_2, which is unknown, but were it to exceed 713 kJ mol^{-1}, when coupled with the error in the estimated *PV* work, the process could be rendered spontaneous.

$$SiO_{2(quartz)} + Xe_{(s)} \rightarrow Si_{(s)} + XeO_{2(g)}$$

$$\Delta H^\circ = 1413 \text{ kJ mol}^{-1} \quad (6)$$

The plausibility of reaction (6) is supported by a recent computational study relating to xenon insertion into SiO_2 networks.[40] This study concluded that xenon could be incorporated into the interstitial spaces of SiO_2 lattices under ambient conditions and that xenon could replace silicon at higher pressures in a two-step process. The initial step requires a substantial amount of energy and involves a redox process in which Si atoms are removed from the lattice and Si−O−O−Si peroxi-linkages are formed (eq 7). The xenon incorporation step (eq 8) has an energy barrier of 177 kJ mol^{-1}.[40]

$$(Si{-}O{-})_2 - Si - (-O{-}Si)_{2(quartz)} \rightarrow 2Si{-}O{-}O{-}Si_{(s)} + Si_{(s)} \quad (7)$$

$$2Si{-}O{-}O{-}Si_{(s)} + Xe_{(s)} \rightarrow (Si{-}O{-})_2 - Xe - (-O{-}Si)_{2(s)} \quad (8)$$

In view of the aforementioned computational results, which support xenon substitution into SiO_2 networks, the previous Raman spectrum of xenon doped SiO_2 obtained from a high-pressure and high-temperature study[10] was re-examined in light of the present findings. The spectrum is consistent with the presence of covalently bound xenon, but the vibrational bands were incorrectly assigned. A band at 588 cm^{-1} was assigned "to the main Raman band of SiO units, located at 596.4 cm^{-1} at room temperature in the gas phase."[10] The reference alluded to by the authors actually quotes SiO stretches ranging from 460.2 to 627.9 cm^{-1} for $(SiO)_n$ ($n = 2-4$) in a solid methane matrix at 25 K.[43] The 588 cm^{-1} band is in good agreement with the experimental frequency for bulk XeO_2 (570.3 cm^{-1}) obtained in the present study and more likely arises from modes whose descriptions approximate $\nu_s(XeO_4)$ and $\nu_{as}(XeO_{2t}{-}XeO_{2t})$. Bands at 814 and 356 cm^{-1} were also previously assigned to XeO_2,[10] but more likely arise from $Si{-}O_{Xe}$ stretching and $O{-}Si{-}O_{Xe}$ bending modes, respectively, where O_{Xe} denotes oxygen bound to xenon. These bands are in good agreement with the E and A_1 modes observed for solid SiO_2 at 795 and 356 cm^{-1}, respectively,[44] and are reassigned accordingly.

CONCLUSION

The present study has provided the synthesis and Raman spectroscopic characterization of macroscopic amounts of XeO_2. Raman spectroscopic studies employing $^{16}O/^{18}O$ isotopic enrichment indicate that XeO_2 possesses an extended structure having a local square-planar XeO_4 geometry around Xe(IV). Xenon dioxide presently represents the only known covalent network structure for a noble-gas compound that exists under near-ambient conditions. The present Raman spectroscopic studies of XeO_2 also correct prior vibrational assignments of xenon-doped SiO_2 containing covalently bound xenon (2.2%) that had been substituted for silicon in a quartz matrix under high-temperature and high-pressure conditions.[10] Such xenon-doped SiO_2 lattices offer the possibility that covalently bound xenon occurs in natural silicates that have been cycled deep into Earth's crust. This could serve to deplete the amount of xenon relative to the lighter noble gases in the atmosphere, providing a plausible explanation for the Earth's missing xenon.

EXPERIMENTAL SECTION

Low-temperature (−150 °C) Raman spectra were recorded in situ in ¼-in. o.d. FEP (perfluoro-ethylene/propylene copolymer) reactors as previously described.[45] Prior to reaction, the reactors were rigorously dried under dynamic vacuum for 24 h and subsequently passivated with F_2 gas for a further 24 h. Under a head of high-purity Ar, 0.400 mL of $H_2{}^{16}O$ (Caledon, HPLC grade) [$H_2{}^{18}O$ (MSD Isotopes, 97.8 atom % ^{18}O); $H_2{}^{16}O/H_2{}^{18}O$; D_2O (MSD Isotopes, 99.8 atom % D)] was syringed into a ¼-in. FEP reactor, which was plugged with a Teflon cap, and cooled to 0 °C in an ice/water bath. Once cooled, the cap was briefly removed and 40−50 mg of crystalline XeF_4[46] was added to the reactor, a few crystals at a time. **NOTE:** *When water was added directly to solid XeF_4, or XeF_4 crystals were added too rapidly, heat generated by the reaction could not be adequately dissipated, resulting in extensive decomposition of XeO_2 to Xe and O_2 which ejected the remaining water and product from the reactor.* A bright, yellow-orange suspension immediately formed upon contact, but upon mixing for ca. 20 s at 0 °C the color of the suspension changed to yellow. The yellow solid was found to be XeO_2 (vide supra), whereas the yellow-orange product was possibly a mixture of molecular XeO_2 and/or lower molecular weight polymorphs resulting from incomplete polymerization. The reactor containing the yellow solid was then placed in an ice/water bath in a centrifuge and centrifuged for 10 s at 7000 rpm at a radial distance of 13 cm. The

sample was removed and immediately quenched at −78 °C and the Raman spectrum was recorded at −150 °C.

■ ASSOCIATED CONTENT

Supporting Information. Hydrolyses of $[Cs][XeOF_3]$ and $XeOF_2$; synthesis of XeO_2 in nonaqueous media; site symmetry analyses for the XeO_4 moiety in the polymeric structure of XeO_2 (Table S1); Natural abundance Raman spectra of yellow-orange, incompletely polymerized product(s) and yellow, macromolecular XeO_2 (Figure S1). This material is available free of charge via the Internet at http://pubs.acs.org.

■ AUTHOR INFORMATION

Corresponding Author
schrobil@mcmaster.ca

■ ACKNOWLEDGMENT

We thank the Natural Sciences and Engineering Research Council of Canada for support in the form of a Discovery Grant (G.J.S.), the Ontario Graduate Scholarship in Science and Technology, and the McMaster Internal Prestige "Ontario Graduate Fellowships" Programs for support (D.S.B.).

■ REFERENCES

(1) Anders, E.; Owen, T. *Science* **1977**, *198*, 453–465.
(2) Ozima, M.; Podosek, F. A. *J. Geophys. Res.* **1999**, *104*, 25493–25499.
(3) Kunz, J.; Staudacher, T.; Allegre, C. J. *Science* **1998**, *280*, 877–880.
(4) Caldwell, W. A.; Nguyen, J. H.; Pfrommer, B. G.; Mauri, F.; Louie, S. G.; Jeanloz, R. *Science* **1997**, *277*, 930–933.
(5) Nishio-Hamane, D.; Yagi, T.; Sata, N.; Fujita, T.; Okada, T. *Geophys. Res. Lett.* **2010**, *37*, L04302.
(6) Wacker, J. F.; Anders, E. *Geochim. Cosmochim. Acta* **1984**, *48*, 2373–2380.
(7) Sill, G. T.; Wilkening, L. L. *Icarus* **1978**, *33*, 13–22.
(8) Matsuda, J.-I.; Matsubara, K. *Geophys. Res. Lett.* **1989**, *16*, 81–84.
(9) Pepin, R. O. *Icarus* **1991**, *92*, 2–79.
(10) Sanloup, C.; Schmidt, B. C.; Chamorro Perez, E. M.; Jambon, A.; Gregoryanz, E.; Mohamed Mezouar, M. *Science* **2005**, *310*, 1174–1177.
(11) Bartlett, N. *Proc. Chem. Soc.* **1962**, 218.
(12) Smith, D. F. *J. Am. Chem. Soc.* **1963**, *85*, 816–817.
(13) Templeton, D. H.; Zalkin, A.; Forrester, J. D.; Williamson, S. M. *J. Am. Chem. Soc.* **1963**, *85*, 817.
(14) Selig, H.; Claassen, H. H.; Chernick, C. L.; Malm, J. G.; Huston, J. L. *Science* **1964**, *143*, 1322–1323.
(15) Huston, J. L.; Studier, M. H.; Sloth, E. N. *Science* **1964**, *143*, 1161–1162.
(16) Gunn, S. R. *J. Am. Chem. Soc.* **1965**, *87*, 2290–2291.
(17) Yamanishi, M.; Hirao, K.; Yamashita, K. *J. Chem. Phys.* **1998**, *108*, 1514–1521.
(18) Bartlett, N.; Rao, P. R. *Science* **1963**, *139*, 506.
(19) Williamson, S. M.; Koch, C. W. *Science* **1963**, *139*, 1046–1047.
(20) Appelman, E. H.; Malm, J. G. *J. Am. Chem. Soc.* **1964**, *86*, 2141–2148.
(21) Williamson, S. M.; Koch, C. W. In *Noble Gas Compounds*; Hyman, H. H., Ed.; University of Chicago Press: Chicago, IL, 1963; pp 149−151.
(22) Ogden, J. S.; Turner, J. J. *Chem. Commun.* **1966**, *19*, 693–694.
(23) Brock, D. S.; Bilir, V.; Mercier, H. P. A.; Schrobilgen, G. J. *J. Am. Chem. Soc.* **2007**, *129*, 3598–3611.
(24) Claassen, H. H.; Knapp, G. *J. Am. Chem. Soc.* **1964**, *86*, 2341–2342.
(25) Tsao, P.; Cobb, C. C.; Claassen, H. H. *J. Chem. Phys.* **1971**, *54*, 5247–5253.
(26) It is possible for a Xe−F stretch to couple with a Xe−O stretch and therefore show an isotopic dependence. However, this possibility was discounted because the corresponding out-of-phase mode was not observed. The latter would produce a second, intense, stretching band at a significantly different frequency in the Xe−F/Xe−O stretching region.
(27) The bands for the symmetric Xe−O−Xe stretch of $[Xe_3OF_3][AsF_6]$, which couple with the terminal Xe−F stretching modes, occur at 419, 430, and 480 cm^{-1}. Because they correspond to a Xe(II) cation, they are among the highest single bond Xe−O stretching frequencies expected for a Xe(II)−O bonded species. Gerken, M.; Moran, M. D.; Mercier, H. P. A.; Pointner, B. E.; Schrobilgen, G. J.; Hoge, B.; Christe, K. O.; Boatz, J. A. *J. Am. Chem. Soc.* **2009**, *131*, 13474–13489.
(28) Gillespie, R. J.; Hargittai, I. *The VSEPR Model of Molecular Geometry*; Allyn and Bacon: Boston, MA, 1991.
(29) Pyykkö, P.; Tamm, T. *J. Phys. Chem. A* **2000**, *104*, 3826–3828.
(30) Nakamoto, K. *Infrared and Raman Spectra of Inorganic and Coordination Compounds, Part A*, 6th ed.; John Wiley & Sons, Inc.: Hoboken, NJ, 2009; pp 278−279 and references therein.
(31) Levy, H. A.; Burns, J. H.; Agron, P. A. *Science* **1963**, *139*, 1208–1209.
(32) Brock, D. S.; Mercier, H. P. A.; Schrobilgen, G. J. *J. Am. Chem. Soc.* **2010**, *132*, 10935–10943.
(33) Turowsky, L.; Seppelt, K. *Z. Anorg. Allg. Chem.* **1992**, *609*, 153–156.
(34) Christe, K. O.; Curtis, E. C.; Dixon, D. A.; Mercier, H. P. A.; Sanders, J. C. P.; Schrobilgen, G. J. *J. Am. Chem. Soc.* **1991**, *113*, 3351–3361.
(35) Boldrini, P.; Gillespie, R. J.; Ireland, P. R.; Schrobilgen, G. J. *Inorg. Chem.* **1974**, *13*, 1690–1694.
(36) McKee, D. E.; Zalkin, A.; Bartlett, N. *Inorg. Chem.* **1973**, *12*, 1713–1717.
(37) Nakamoto, K. *Infrared and Raman Spectra of Inorganic and Coordination Compounds, Part A*, 6th ed.; John Wiley & Sons, Inc.: Hoboken, NJ, 2009; pp 129−134.
(38) Alternatively, one of the two bands at 227.9 and 239.1 cm^{-1} may result from the extended lattice. Rotational modes that are otherwise unobserved for free XeF_4 may be observed in a XeO_2 network structure. A site symmetry analysis (see the Supporting Information) indicates that a doubly degenerate E-mode originating from a rotational mode is rendered Raman active upon symmetry lowering from D_{4h} to D_{2d} in an extended structure and could account for the presence of one of the aforementioned bands.
(39) Gerken, M.; Schrobilgen, G. J. *Inorg. Chem.* **2002**, *41*, 198–204.
(40) Probert, M. I. J. *J. Phys.: Condens. Matter* **2010**, *22*, 025501.
(41) Chase, M. W. Jr. *NIST JANAF Thermochemical Tables*; American Institute of Physics: New York, 1998.
(42) Schwalbe, L. A.; Crawford, R. K.; Chen, H. H.; Aziz, R. A. *J. Chem. Phys.* **1977**, *66*, 4493–4502.
(43) Friesen, M.; Junker, M.; Zumbusch, A.; Schnöckel, H. *J. Chem. Phys.* **1999**, *111*, 7881–7887.
(44) Ranieri, V.; Bourgogne, D.; Darracq, S.; Cambon, M.; Haines, J.; Cambon, O.; Leparc, R.; Levelut, C.; Largeteau, A.; Demazeau, G. *Phys. Rev. B* **2009**, *79*, 224304.
(45) Casteel, W. J., Jr.; Dixon, D. A.; Mercier, H. P. A.; Schrobilgen, G. J. *Inorg. Chem.* **1996**, *35*, 4310–4322.
(46) Chernick, C. L.; Malm, J. G. *Inorg. Synth.* **1966**, *8*, 254–258.